Detection of CISO with time-resolved Fourier-transform infrared absorption spectroscopy

Li-Kang Chu, Yuan-Pern Lee, and Eric Y. Jiang

Citation: The Journal of Chemical Physics **120**, 3179 (2004); doi: 10.1063/1.1641007
View online: http://dx.doi.org/10.1063/1.1641007
View Table of Contents: http://scitation.aip.org/content/aip/journal/jcp/120/7?ver=pdfcov
Published by the AIP Publishing

Detection of ClSO with time-resolved Fourier-transform infrared absorption spectroscopy

Li-Kang Chu
Department of Chemistry, National Tsing Hua University, Hsinchu 30013, Taiwan

Yuan-Pern Lee[a)]
Department of Chemistry, National Tsing Hua University, Hsinchu 30013, Taiwan, and Institute of Atomic and Molecular Sciences, Academia Sinica, Taipei, Taiwan

Eric Y. Jiang
Thermo Electron Corporation, Madison, Wisconsin 53711

(Received 31 October 2003; accepted 20 November 2003)

ClSO was produced as an intermediate upon irradiating a flowing mixture of Cl_2SO and Ar with a KrF excimer laser at 248 nm. A step-scan Fourier-transform infrared spectrometer coupled with a small multipass absorption cell was employed to detect time-resolved absorption spectrum of ClSO. A transient spectrum in the region 1120–1200 cm^{-1}, which diminished on prolonged reaction, is assigned to the S–O stretching (ν_1) mode of ClSO. A spectrum with a resolution of 0.3 cm^{-1} partially reveals rotational structure with the *Q*-branch at 1162.9 cm^{-1}. Calculations with density-functional theory (B3LYP/aug-cc-pVTZ) predict the geometry, vibrational, and rotational parameters of ClSO. An IR absorption spectrum of ClSO simulated based on predicted rotational parameters agrees satisfactorily with experimental results. ClSO produced from photolysis of Cl_2SO at 248 nm is internally hot. © *2004 American Institute of Physics.* [DOI: 10.1063/1.1641007]

INTRODUCTION

Thionyl chloride (Cl_2SO) is commonly used in organic syntheses and serves also as an excellent ligand coupling reagent.[1] In high-capacity lithium batteries it promotes cycling efficiencies of alkali metals in electrolytes.[2] The photodissociation dynamics of Cl_2SO have been investigated extensively because of the importance in understanding the competition among processes involving concerted and stepwise three-body dissociation, and two-body dissociation; dissociation products SO and Cl can be probed readily.[3–10]

UV absorption[11] of Cl_2SO shows an onset ~300 nm and two maxima near 194 nm ($\sigma = 1.3\times10^{-17}$ cm^2) and 244 nm ($\sigma = 7.1\times10^{-18}$ cm^2), corresponding to transitions $\sigma^*_{S-Cl} \leftarrow n_{Cl}$ and a combination of $\sigma^*_{S-Cl} \leftarrow n_S$ and $\sigma^*_{S-O} \leftarrow n_S$, respectively; the symbol * indicates antibonding orbitals.[4,10] At 193 nm, the major channel for photodissociation involves a concerted three-body dissociation,

$$Cl_2SO \rightarrow 2Cl + SO, \tag{1}$$

accounting for more than 80% of the overall decay.[7,8] The two-body Cl-elimination channel,

$$Cl_2SO \rightarrow ClSO + Cl, \tag{2}$$

has a branching ratio ~17%, whereas the molecular-elimination channel

$$Cl_2SO \rightarrow Cl_2 + SO \tag{3}$$

is less than 3%. About one-fifth of SO produced in channel (1) is electronically excited in the $a\,^1\Delta$ state;[5] the ground $X\,^3\Sigma^-$ state of SO ($v \leqslant 6$) is vibrationally inverted at $v = 2$ or 3.[6,7] At 248 nm, the Cl-elimination channel dominates (>96.5%), whereas the molecular-elimination channel yielding SO predominantly in the $b\,^1\Sigma^+$ state accounts for only ~3.5%; the three-body dissociation channel has an insignificant contribution.[7,8] ClSO produced in reaction (2) undergoes further dissociation

$$ClSO \rightarrow Cl + SO \tag{4}$$

to form Cl and SO with an isotropic angular distribution.[8] Employing the REMPI (resonance-enhanced multiphoton ionization)–TOF (time-of-flight) technique to probe SO and Cl, Roth *et al.*[10] found that photodissociation of Cl_2SO at 235 nm proceeds via two potential-energy surfaces A'' and A'. Dissociation on the A'' surface produces Cl ($^2P_{3/2}$) and Cl ($^2P_{1/2}$) in nearly equal proportions in conjunction with SOCl radical which carries about half the available energy as internal energy, whereas dissociation on the A' surface produces mainly 2Cl+SO via sequential three-body decay. Although these investigations of photodissociation dynamics involved laser-induced fluorescence (LIF),[6,7] REMPI,[10] and diode-laser absorption[5] techniques to probe Cl and SO, no direct spectral detection of ClSO has been reported. ClSO was probed only with a mass spectrometer in an investigation using photofragment translational spectroscopy, but only about one-fifth of ClSO survived electron bombardment.[8]

ClSO has been characterized with electron paramagnetic resonance (EPR),[12] far infrared laser magnetic resonance,[13] and microwave spectroscopy.[14] Li predicted geometries, vibrational frequencies, and energies of ClSO in both its ground ($X\,^2A''$) and first electronically excited states ($A\,^2A'$) using various quantum-chemical calculation

a)Author to whom correspondence should be addressed. Electronic mail: yplee@mx.nthu.edu.tw

methods.[15] Vibrational wave numbers of the $X\,^2A''$ state of ClSO are predicted to be ν_1 (S–O stretch) = 1099 cm^{-1}, ν_2 (Cl–S stretch) = 477 cm^{-1}, and ν_3 (ClSO bend) = 294 cm^{-1}. To our knowledge, no vibrational spectrum of ClSO has been reported. Hence it would be interesting to develop an infrared detection technique to investigate further the photodissociation dynamics of Cl_2SO and reaction kinetics involving ClSO.

We recently coupled a step-scan Fourier-transform spectrometer with a multipass absorption cell to record time-resolved infrared (IR) absorption spectra of reaction intermediates or vibrationally excited species in the gas phase.[16–18] Compared with time-resolved Fourier-transform spectroscopy (TR–FTS) in emission mode,[19–25] TR–FTS in absorption mode provides additional information on nonemitting states or species, particularly on molecules in their ground vibrational state. Here we report an application of step-scan TR–FTS to record IR absorption spectra of the intermediate ClSO upon photodissociation of Cl_2SO.

EXPERIMENTAL SECTION

A commercial step-scan Fourier-transform spectrometer (Bruker, IFS66v/S or Thermo Nicolet Nexus 870) operating in absorption mode is employed.[16,17] A White cell with a base path length of 20 cm and a maximal effective path length of 8 m was placed in the sample compartment of the spectrometer; the volume of the cell is ~1600 cm^3. The housing of the White cell was modified to accommodate two rectangular (3×12 cm^2) quartz windows to pass photolysis beams that propagate perpendicular to multipassing IR beams. The photolysis laser beam passes these quartz windows and is multiply reflected between a pair of rectangular laser mirrors installed externally but parallel to the quartz windows. A KrF excimer laser (Lambda Physik, LPX110i, 21 Hz) emitting at 248 nm is employed for photodissociation; typical energy employed is ~85 mJ $pulse^{-1}$ with a beam dimension $\sim6\times11$ mm^2. The efficiency of photolysis of Cl_2SO is estimated to be ~50% based on the absorption cross section of Cl_2SO at 248 nm ($\sim7\times10^{-18}$ cm^2 $molecule^{-1}$),[11] the effective path length ~17 cm, and the laser fluence $\sim1.6\times10^{17}$ photons cm^{-2}. Flow rates are $F_{Cl_2SO}=0.29-0.57$ and $F_{Ar}=2.46-19.2$ STP cm^3 s^{-1}; STP denotes standard temperature (273.15 K) and pressure (1 atm). The total pressure was 1.85–29.7 Torr, with partial pressure of Cl_2SO in the range 0.35–0.65 Torr.

Derivation of time-resolved difference absorption spectra from interferograms recorded with ac- and dc-coupled signals is described previously.[16,26] After preamplification, the ac-coupled signal from the MCT detector (Kolmar, Model KMPV11-1-J2, 20 MHz) was further amplified (Stanford Research Systems, Model SR560, using bandwidth 300–1 MHz) 10 times, whereas the dc-coupled signal was not further amplified before being sent to the internal 16-bit digitizer (2×10^5 sample s^{-1}) of the spectrometer. Typically, 200 data points were acquired at 5 μs intervals after photolysis; the signal is typically averaged over 60 laser shots at each scan step. Proper optical filters serve to define a small spectral region so that undersampling decreases the number of data points, hence the duration of data acquisition. For survey spectra in the range 960–1430 cm^{-1} at a resolution of 2.5 cm^{-1}, 516 scan steps were completed within an acquisition period ~25 min, whereas for high-resolution spectra in the range 1050–1370 cm^{-1} at a resolution 0.3 cm^{-1} data acquisition with 2214 scan steps requires ~110 min.

At the later stage of experiments, a new step-scan spectrometer (Thermo Nicolet, Nexus 870) with a fast MCT detector (20 MHz) was employed. The spectrometer controls mirror positions to within ±0.2 nm (Ref. 27) and is equipped with a 14-bit digitizer (Gage Applied Technology, CompuScope 14100, 10^8 sample s^{-1}). Typically, 150 data points were acquired at 1 μs integrated intervals (100 dwells at 10 ns gate width) after photolysis; the signal is typically averaged over 60 laser shots at each scan step. With its present software, the data acquisition time is typically about 30% greater than that with Bruker spectrometer, but the ratio of signal to noise appears to be superior to previous measurements. For survey spectra in the range 850–1500 cm^{-1} at a resolution of 1.5 cm^{-1}, 1200 scan steps were completed within ~70 min, whereas for high-resolution spectra in the range 1050–1343 cm^{-1} at a resolution 0.3 cm^{-1} data acquisition with 2592 scan steps requires ~170 min.

Cl_2SO (>99%, Fluka Chemika) and Ar (99.9995%, AGA Specialty Gases) were used without further purification.

THEORETICAL CALCULATIONS

The equilibrium geometry, vibrational frequencies, and IR intensities were calculated with B3LYP density-functional theory using the GAUSSIAN 98 program.[28] The B3LYP method uses Becke's three-parameter hybrid exchange functional with a correlation functional of Lee, Yang, and Parr.[29,30] Dunning's correlation-consistent polarized-valence triple-zeta basis set, augmented with *s*, *p*, *d*, and *f* functions (aug-cc-pVTZ)[31,32] was applied in these calculations. Analytic first derivatives were utilized in geometry optimization, and vibrational frequencies were calculated analytically at each stationary point.

Calculated geometry, rotational parameters, vibrational wave numbers, and IR intensities are compared with those of previous work in Table I. The structure and rotational axes are shown in Fig. 1(A). The Cl–S bond length of 2.099 Å predicted in this work is slightly greater than those predicted previously with QCISD/6-31G* (2.088 Å) and MP2/6-31G* (2.092 Å), but smaller than that (2.119 Å) predicted with MP2/6-311G(2d).[15] The predicted S–O bond length of 1.479 Å is smaller than the value 1.499 Å predicted with QCISD/6-31G*, but greater than values 1.457 and 1.449 Å predicted with MP2/6-31G* and MP2/6-311G(2d), respectively. The predicted bond angle of 109.9° is similar to the value 109.3° predicted with QCISD/6-31G*, but much smaller than those predicted with MP2. The difference in geometry results in variations of rotational parameters less than 9% for the *A* parameter, and 3% for the *B* and *C* parameters, as listed in Table I. Rotational spectral parameters predicted in this work are smaller by ~4% than those derived with microwave spectroscopy.[14]

TABLE I. Comparison of geometry and vibrational wave numbers of ^{35}ClSO derived from various theoretical calculations.

	Experiment	B3LYP /aug-cc-pVTZ	QCISD /6-31G*	MP2 /6-31G*	MP2 /6-311G(2d)
r_{Cl-S}/Å	2.090[a]	2.099	2.088	2.092	2.119
r_{S-O}/Å	1.418[a]	1.479	1.499	1.457	1.449
∠ClSO/deg	107.8[a]	109.9	109.3	112.6	112.1
A/cm^{-1}	1.094 73	1.061 51	1.0280	1.1566	1.1478
B/cm^{-1}	0.151 88	0.145 67	0.1469	0.1439	0.1419
C/cm^{-1}	0.133 17	0.128 09	0.1285	0.1280	0.1263
ν_1/cm^{-1}	1162.9[b]	1156.1 (90.6)[c]	1099 (48)[c,d]		
ν_2/cm^{-1}		467.0 (97.1)	477 (100)		
ν_3/cm^{-1}		291.2 (2.9)	294		
Reference	14	This work	15	15	15

[a]The geometry is derived by assuming a bond angle of 107.8°. If a bond angle of 109.9° is used, r_{Cl-S} = 2.055 Å and r_{S-O} = 1.479 Å.
[b]This work.
[c]IR intensities (in km mol^{-1}) are listed in parentheses.
[d]IR intensities relative to the most intense band (set to 100).

The smaller S–O bond length calculated with B3LYP/aug-cc-pVTZ is consistent with a larger wave number (1156 cm^{-1}) predicted for the S–O stretching mode, as compared with a value of 1099 cm^{-1} predicted with QCISD/6-31G*. Predictions of vibrational wave numbers for the S–O stretch using B3LYP/aug-cc-pVTZ are estimated to be accurate to within 1%, based on results of SSO (calculated 1169.0 cm^{-1}, gas phase 1166.5 cm^{-1}),[33,34] c-OSNO (calculated 1153.3 cm^{-1}, N_2 matrix 1156.1 cm^{-1}), and t-OSNO (calculated 1173.3 cm^{-1}, N_2 matrix 1178.0 cm^{-1}).[35] If we use the same ratio of experimental to calculated wave numbers for FSO, 1215/1165=1.043, reported by Li using identical method, we derive a revised value of 1146 cm^{-1} for the S–O stretching mode based on a value 1099 cm^{-1} calculated with QCISD/6-31G*; this revised value is only ~1% smaller than our predicted value of 1156 cm^{-1}. Hence, we expect that the vibrational wave number for the S–O stretching mode of ClSO is likely in the range 1146–1166 cm^{-1}. Predicted displacement vectors for the S–O stretching (ν_1) mode and the associated dipole derivative is shown in Fig. 1(B). Wave numbers predicted in this work for the other two vibrational modes, 467 cm^{-1} for Cl–S stretching and 291 cm^{-1} for ClSO-bending modes, are similar to those reported previously, but are beyond our range of detection.

EXPERIMENTAL RESULTS AND DISCUSSION

As a test, conventional cw measurements were performed with a static cell containing 0.110 Torr of Cl_2SO. Traces (A) and (B) of Fig. 2 represent partial IR absorption spectra at a resolution of 0.25 cm^{-1} recorded before and after laser irradiation at 248 nm (20 Hz) for 60 s, respectively. Cl_2SO absorption is characterized by an intense band near 1251.6 cm^{-1} (ν_1, S–O stretch).[36] Absorption of SO_2 as the end product is clearly visible in the region 1300–1400 (intense) and 1100–1200 cm^{-1} (weak); these absorption bands are consistent with previous literature values for the asym-

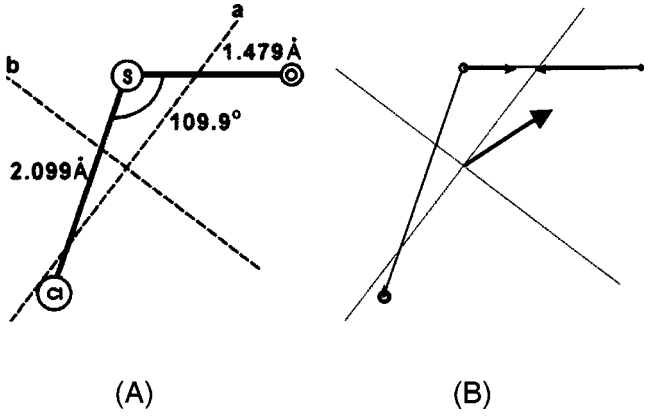

FIG. 1. Molecular structure and rotational axes of ClSO (A), and displacement vectors for the S–O stretching (ν_1) mode and associated dipole derivative of ClSO (B) predicted with the B3LYP/aug-cc-pVTZ method. Bond lengths are in Å and bond angle is in degree.

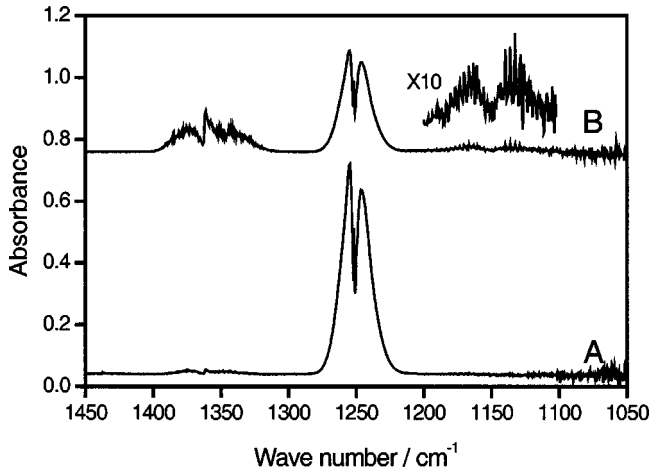

FIG. 2. Survey cw IR absorption spectra of Cl_2SO (0.110 Torr) in a static cell. (A) before irradiation; (B) after laser irradiation at 248 nm for 60 s (20 Hz, 100 mJ cm^{-2}). Path length is 6.4 m and resolution is 0.25 cm^{-1}.

metric (1361.8 cm^{-1}) and symmetric (1151.4 cm^{-1}) S–O stretching modes of SO_2.[37] No absorption band in the static-cell experiment may be ascribed to ClSO.

Spectra of internally excited Cl_2SO

A representative three-dimensional (3D) plot of temporally resolved survey difference spectra at 2 μs intervals after laser irradiation of a flowing mixture of Cl_2SO/Ar (≅1/4.2, 1.85 Torr) at 248 nm is shown in Fig. 3(A) (resolution 1.5 cm^{-1}). In these difference spectra, features pointing up indicate production, whereas those pointing down indicate destruction. The downward features near 1251 cm^{-1} is due to loss of parent molecules. A new feature in the spectral range 1120–1200 cm^{-1} appears immediately after irradiation, then decays with time; it will be discussed in the next section.

On each side of the downward parent band, more pronounced on the smaller wave number side, there are new features pointing upward, then decays with time. These new features are readily assigned as absorption of Cl_2SO parent in highly excited rotational and vibrational levels, which were produced via internal conversion from the initially prepared electronically excited state; a population greater than thermal distribution before photolysis yields upward absorption features. We found that such upward features on both sides of absorption bands of the parent are a common observation in the absorption spectrum of a photolyzed species after irradiation. In many cases these two side-lobes interfere with nearby absorption bands of dissociation products and hamper their detection.

Figure 3(B) shows a representative 3D plot for spectra recorded at 2 μs intervals after photolysis of Cl_2SO (0.355 Torr) and excessive Ar (24.35 Torr) in a flowing mixture. In the 1200–1300 cm^{-1} region where Cl_2SO absorbs, the upward side-lobes due to increase in populations of internally excited states diminish and the width of the downward feature decreases, because of efficient relaxation under high pressure.

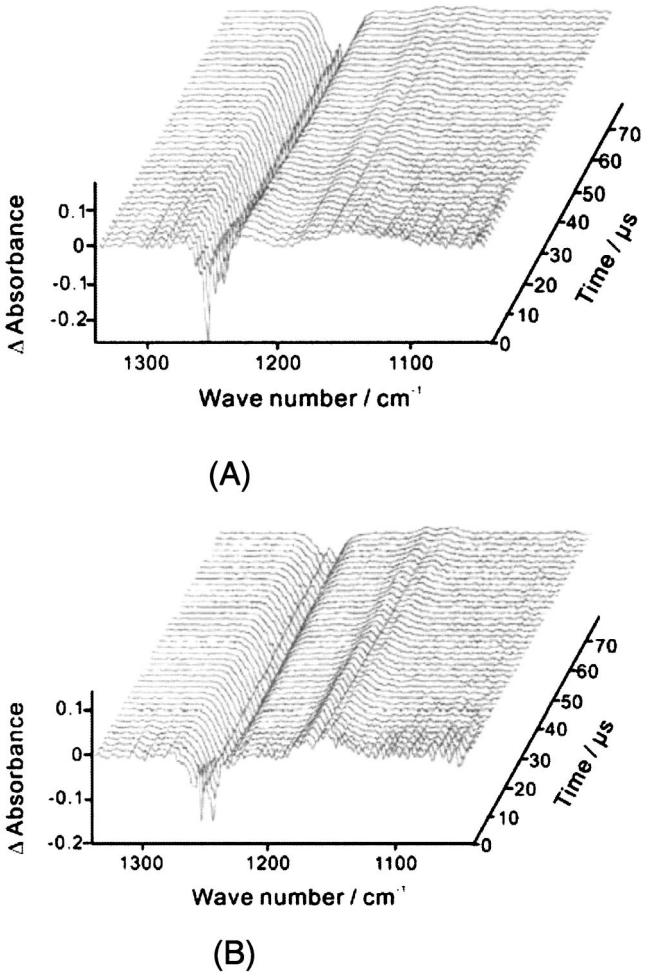

FIG. 3. Time-resolved survey IR absorption spectra of a flowing mixture of Cl_2SO/Ar upon photolysis at 248 nm (21 Hz, 150 mJ cm^{-2}) displayed in three-dimensional mode. (A) 1.85 Torr, Cl_2SO/Ar= 1/4.2; (B) 24.71 Torr, Cl_2SO/Ar= 1/69. Path length is 6.4 m and resolution is 1.5 cm^{-1}. Traces start at 2 μs after irradiation and are separated at 2-μs intervals.

Spectra of ClSO

Even though the two-body dissociation channel [reaction (2)] dominates photodissociation of Cl_2SO at 248 nm, ClSO produced upon photolysis is internally excited so that a substantial portion undergoes further dissociation to form Cl and SO.[7,8,10] In order to quench the internal excitation and stabilize ClSO, we added excessive Ar in the system. The 3D plots shown in Figs. 3(A) and 3(B) for spectra recorded after photolysis of Cl_2SO and Ar indicates an enhanced peak intensity with narrower widths for the new feature in the 1135–1190 cm^{-1} region when excessive Ar was added.

Transient absorption spectra with an improved resolution of 0.3 cm^{-1} were recorded upon irradiation of a flowing mixture containing Cl_2SO/Ar(1/45) at 29.7 Torr; the spectrum averaged over 10–40 μs after photolysis is shown in trace(A) of Fig. 4. The *Q* branch is clearly resolved from *P* and *R* branches, but rotational structures of *P* and *R* branches are unresolved. No satisfactory spectrum at resolutions better than 0.3 cm^{-1} was obtained because the ratio of signal to noise decreases and the duration of data acquisition increases substantially.

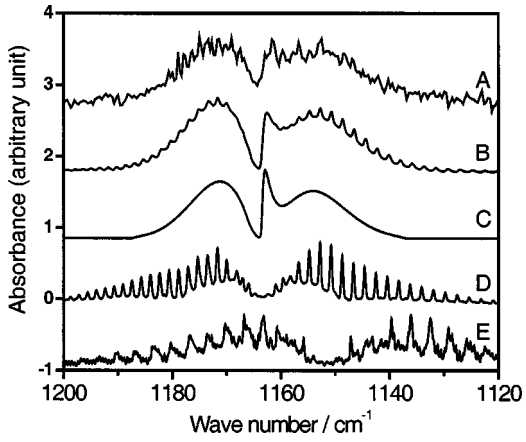

FIG. 4. Comparison of observed absorption spectrum of ClSO and simulated spectra; (A) spectrum at resolution 0.3 cm^{-1} and integrated for 10–40 μs after 248-nm laser irradiation (21 Hz, 130 mJ cm^{-2}) of a flowing mixture of Cl_2SO/Ar= 1/45 at 29.7 Torr; (B) simulated spectra based on rotational parameters obtained from microwave spectra (Ref. 14); see text; (C) *a*-type component; (D) *b*-type component; (E) spectrum of SO_2 at 298 K (from Hitran database) (Ref. 39).

The wave number of the maximum of the *Q* branch, 1162.9 cm^{-1}, is within the expected range, 1146–1166 cm^{-1}, for the S–O stretching mode of ClSO, and close to the value of 1156 cm^{-1} predicted with the B3LYP/aug-cc-pVTZ method. Although the SO product also absorbs in this region, observed new features are not due to SO because SO absorbs at 1137.9 cm^{-1} (Ref. 38). The observed transient absorption spectrum fits poorly with the spectrum of the end product SO_2 which absorbs at 1361.8 and 1151.4 cm^{-1}; spectrum of the band at 1151.4 cm^{-1} is shown in trace (E) of Fig. 4 for comparison.[39] Considering that observed peak wave numbers are near that predicted for ClSO with theory but not for other possible products SO and SO_2, and that these new features were enhanced at high pressures, we conclude that the observed transient absorption is likely due to ClSO.

Simulation of the ν_1 absorption band of ClSO

As it is unlikely to derive rotational parameters from observed spectra with the present spectral resolution, we simulate the band contour to compare with observed spectra. Rotational axes *a* and *b* of ClSO are shown in Fig. 1(A); the *c* axis is perpendicular to the molecular plane. Because the S–O stretching mode alters the dipole moment mainly along the *a*-axis, *a*-type absorption lines are expected to be dominant. The projection of the displacement vector onto *a* and *b* axes are 0.78:1.00, whereas the projection of the dipole derivative onto these axes are 1.00:0.35.

The spectrum at 350 K was simulated with the SPECVIEW program[40] using rotational parameters *A*, *B*, and *C* derived from microwave experiments,[14] $J_{max}=120$, and a Doppler line shapes with FWHM=0.3 cm^{-1}. Contributions from ^{37}ClSO are also included even though the ^{37}Cl-isotopic shift for the S–O stretching mode is small. Ratios of rotational parameters of the upper ($v=1$) and the lower ($v=0$) state (A'/A'', B'/B'', and C'/C'') are estimated to be 0.9906, 0.9993, and 0.9982; relative ratios of these values are determined according to the displacement vector of the S–O stretch, and the A'/A'' value is varied to derive the best fit. Simulated *a*-type and *b*-type spectra are shown in traces (C) and (D) of Fig. 4, respectively. A simulated spectrum of ClSO using a ratio of 1.00:0.35 for *a*-type and *b*-type components is shown in trace (B); it agrees satisfactorily with experimental observation in trace (A), with most characteristic features reproduced.

A comparison of spectra averaged 10–20 μs after laser irradiation and under a total pressure of 4.76 Torr [Cl_2SO/Ar=1/8.5, trace (A)] and 22.50 Torr [Cl_2SO/Ar =1/44, trace (B)] is shown in Fig. 5. The new feature recorded at 22.50 Torr fits well with a simulated rotational distribution corresponding to 350 K, whereas that recorded at 4.76 Torr is internally hot. The *R*-band contour is consistent with a simulated rotational distribution with a temperature ~700 K, but the *P*-band contour is redshifted by ~10 cm^{-1} from the simulated one, indicating the existence of vibrationally excited states of ClSO. Because the vibrational anharmonicity of ClSO is unknown, we are unable to estimate the extent of vibrational excitation.

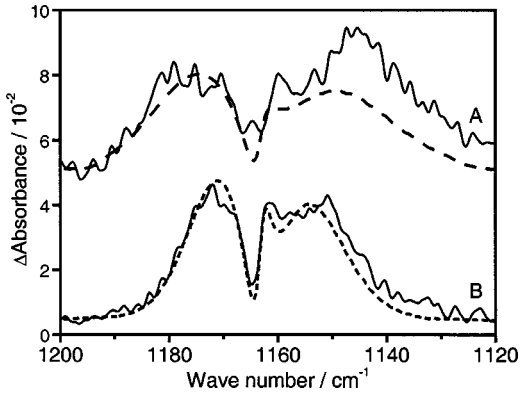

FIG. 5. Comparison of transient absorption spectra averaged over 10–20 μs after 248 nm irradiation of Cl_2SO; (A) 4.76 Torr, Cl_2SO/Ar=1/8.5; (B) 22.50 Torr, Cl_2SO/Ar=1/44. Pathlength is 6.4 m and resolution is 1.0 cm^{-1}.

CONCLUSION

We demonstrate an application of using time-resolved Fourier-transform absorption technique to detect the S–O stretching band of the transient species ClSO upon photolysis of gaseous Cl_2SO. Although current detectivity limits the resolution to 0.3 cm^{-1} in this experiment so that fully resolved rotational spectrum is unavailable, our spectrum conforms satisfactorily to a simulation based on rotational parameters derived from microwave spectroscopy; the vibrational wave number is also consistent with that for the S–O stretching mode of ClSO predicted with theoretical calculations. Spectrum recorded at low pressure indicates that ClSO is internally excited. This band might be probed directly in future chemical-kinetic experiments on reactions involving ClSO if there is no interference from SO_2.

ACKNOWLEDGMENTS

We thank the National Science Council of Taiwan (Grant No. NSC92-2113-M-007-034) and MOE Program for Promoting Academic Excellence of Universities (Grant No. 89-FA04-AA) for support, and V. Stakhursky and T. A. Miller for providing the SpecView software for spectral simulation.

[1] S. Oae, Y. Inubushi, and M. Yoshihara, Phosphorus, Sulfur Silicon Relat. Elem. **103**, 101 (1995).
[2] J. Fuller, R. A. Osteryoung, and R. T. Carlin, J. Electrochem. Soc. **142**, 3632 (1995) and references therein.
[3] R. J. Donovan, D. Husain, and P. T. Jackson, Trans. Faraday Soc. **65**, 2930 (1969).
[4] M. Kawasaki, K. Kasatani, H. Sato, H. Shinohara, N. Nishi, H. Ohtoshi, and I. Tanaka, Chem. Phys. **91**, 285 (1984).
[5] H. Kanamori, E. Tiemann, and E. Hirota, J. Chem. Phys. **89**, 621 (1988).
[6] X. Chen, F. Asmar, H. Wang, and B. R. Weiner, J. Phys. Chem. **95**, 6415 (1991).
[7] H. Wang, X. Chen, and B. R. Weiner, J. Phys. Chem. **97**, 12260 (1993).
[8] G. Baum, C. S. Effenhauser, P. Felder, and J. R. Huber, J. Phys. Chem. **96**, 756 (1992).
[9] B. C. Stuart, S. M. Cameron, and H. T. Powell, Chem. Phys. Lett. **191**, 273 (1992).
[10] M. Roth, C. Maul, and K.-H. Gericke, Phys. Chem. Chem. Phys. **4**, 2932 (2002).
[11] A. P. Uthman, P. J. Demlein, T. D. Allston, M. C. Withiam, M. J. McClements, and G. A. Takacs, J. Phys. Chem. **82**, 2252 (1978).
[12] K. Nishikida and F. Williams, J. Magn. Reson. (1969–1992) **14**, 348 (1974).

[13] H. E. Radford, F. D. Wayne, and J. M. Brown, J. Mol. Spectrosc. **99**, 209 (1983).
[14] S. Saito, Y. Endo, and E. Hirota, Annual Review of Institute of Molecular Sciences, Japan, Paper II-A-12, 1980, p. 47.
[15] Z. Li, J. Phys. Chem. A **101**, 9545 (1997).
[16] J. Eberhard, P.-S. Yeh, and Y.-P. Lee, J. Chem. Phys. **107**, 6499 (1997).
[17] S.-H. Chen, L.-K. Chu, Y.-J. Chen, I-C. Chen, and Y.-P. Lee, Chem. Phys. Lett. **333**, 365 (2001).
[18] Y.-J. Chen, L.-K. Chu, S.-R. Lin, and Y.-P. Lee, J. Chem. Phys. **115**, 6513 (2001).
[19] P.-S. Yeh, G.-H. Leu, Y.-P. Lee, and I-C. Chen, J. Chem. Phys. **103**, 4879 (1995).
[20] S.-R. Lin and Y.-P. Lee, J. Chem. Phys. **111**, 9233 (1999).
[21] S.-R. Lin, S.-C. Lin, Y.-C. Lee, Y.-C. Chou, I-C. Chen, and Y.-P. Lee, J. Chem. Phys. **114**, 160 (2001).
[22] S.-R. Lin, S.-C. Lin, Y.-C. Lee, Y.-C. Chou, I-C. Chen, and Y.-P. Lee, J. Chem. Phys. **114**, 7396 (2001).
[23] C.-Y. Wu, C.-Y. Chung, Y.-C. Lee, and Y.-P. Lee, J. Chem. Phys. **117**, 9785 (2002).
[24] C.-Y. Wu, Y.-P. Lee, J. F. Ogilvie, and N. S. Wang, J. Phys. Chem. A **107**, 2389 (2003).
[25] K.-S. Chen, S.-S. Cheng, and Y.-P. Lee, J. Chem. Phys. **119**, 4229 (2003).
[26] W. Uhmann, A. Becker, C. Taran, and F. Siebert, Appl. Spectrosc. **45**, 390 (1991).
[27] E. Y. Jiang, Spectroscopy (Eugene, Or.) **17**, 22 (2002).
[28] M. J. Frisch, G. W. Trucks, H. B. Schlegel *et al.*, GAUSSIAN 98, Revision A.9, Gaussian Inc., Pittsburgh, PA, 1998.
[29] A. D. Becke, J. Chem. Phys. **98**, 5648 (1993).
[30] C. Lee, W. Yang, and R. G. Parr, Phys. Rev. B **37**, 785 (1988).
[31] T. H. Dunning, Jr., J. Chem. Phys. **90**, 1007 (1989).
[32] D. E. Woon and T. H. Dunning, Jr., J. Chem. Phys. **98**, 1358 (1993).
[33] W.-J. Lo, Y.-J. Wu, and Y.-P. Lee, J. Chem. Phys. **117**, 6655 (2002).
[34] J. Lindenmayer and H. J. Jones, J. Mol. Spectrosc. **112**, 71 (1985).
[35] M. Bahou and Y.-P. Lee, J. Chem. Phys. **115**, 10694 (2001).
[36] T. Shimanouchi, J. Phys. Chem. Ref. Data **6**, 993 (1977).
[37] K. Kim and W. T. King, J. Chem. Phys. **80**, 969 (1984).
[38] C. Clerbaux and R. Colin, J. Mol. Spectrosc. **165**, 334 (1994).
[39] L. S. Rothman, C. P. Rinsland, A. Goldman *et al.*, J. Quant. Spectrosc. Radiat. Transf. **60**, 665 (1998).
[40] V. Stakhursky and T. A. Miller, SpecView: Simulation and Fitting of Rotational Structure of Electronic and Vibronic Bands, 56th OSU International Symposium on Molecular Spectroscopy, Columbus, Ohio, 2001.